# Nonlinear Dynamics: Part 2

Andy Wolski

The Cockcroft Institute, and the University of Liverpool, UK

**CAS: Introduction to Accelerator Physics**
**Budapest, Hungary**
**October 2016**

In these two lectures on nonlinear dynamics, we shall introduce a number of topics:

- Mathematical tools for modelling nonlinear dynamics:
  – *power series (Taylor) maps; symplectic maps.*

- Effects of nonlinear perturbations:
  – *resonances; tune shifts; dynamic aperture.*

- Analysis methods:
  – *normal form analysis; frequency map analysis.*

We shall discuss these aspects of the subject in the context of two types of accelerator system:

1. a bunch compressor (a single-pass system);

2. a storage ring (a multi-turn system).

Our aim is to provide an introduction to some of the key concepts of nonlinear dynamics in particle accelerators.

In the first lecture, we:

- described some of the sources of nonlinearities in particle accelerators;

- applied power series representations of transfer maps to model the nonlinear dynamics in a bunch compressor (an example of a single-pass accelerator system).

- investigated the significance and potential impact of nonlinear dynamics in a bunch compressor;

By the end of this second lecture, you should be able to:

- describe some of the phenomena associated with nonlinearities in periodic beamlines (such as storage rings);
- explain the significance of *symplectic maps*, and describe some of the challenges in calculating and applying symplectic maps;
- outline some of the analysis methods that can be used to characterise nonlinear beam dynamics in periodic beamlines.

## Example of a periodic system: a simple storage ring

As an example, let us consider the transverse dynamics in a simple storage ring. We shall assume that:

- The storage ring is constructed from some number of identical cells consisting of dipoles, quadrupoles and sextupoles.
- The phase advance per cell can be tuned from close to zero, up to about $0.5 \times 2\pi$.
- There is one sextupole per cell, which is located at a point where the horizontal beta function is 1 m, and the alpha function is zero.

Usually, storage rings will contain (at least) two sextupoles per cell, to correct horizontal and vertical chromaticity. To keep things simple, we will use only one sextupole per cell.

Sextupoles are needed in a storage ring to compensate for the fact that quadrupoles have lower focusing strength for particles of higher energy:

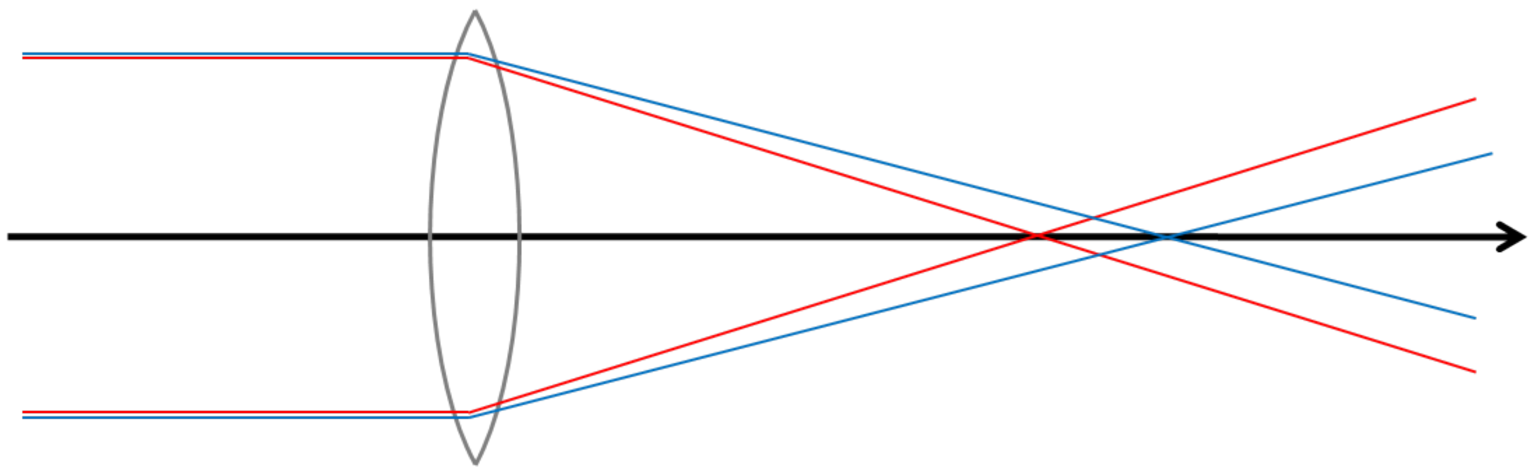

The change in focusing strength with particle energy has undesirable consequences, especially in storage rings: it can lead to particle motion becoming unstable because of resonances.

# A reminder: correcting chromaticity with sextupoles

A sextupole can be regarded as a quadrupole with focusing strength that increases with horizontal offset from the axis.

If sextupoles are located where there is non-zero dispersion, they can be used to control the chromaticity in a storage ring.

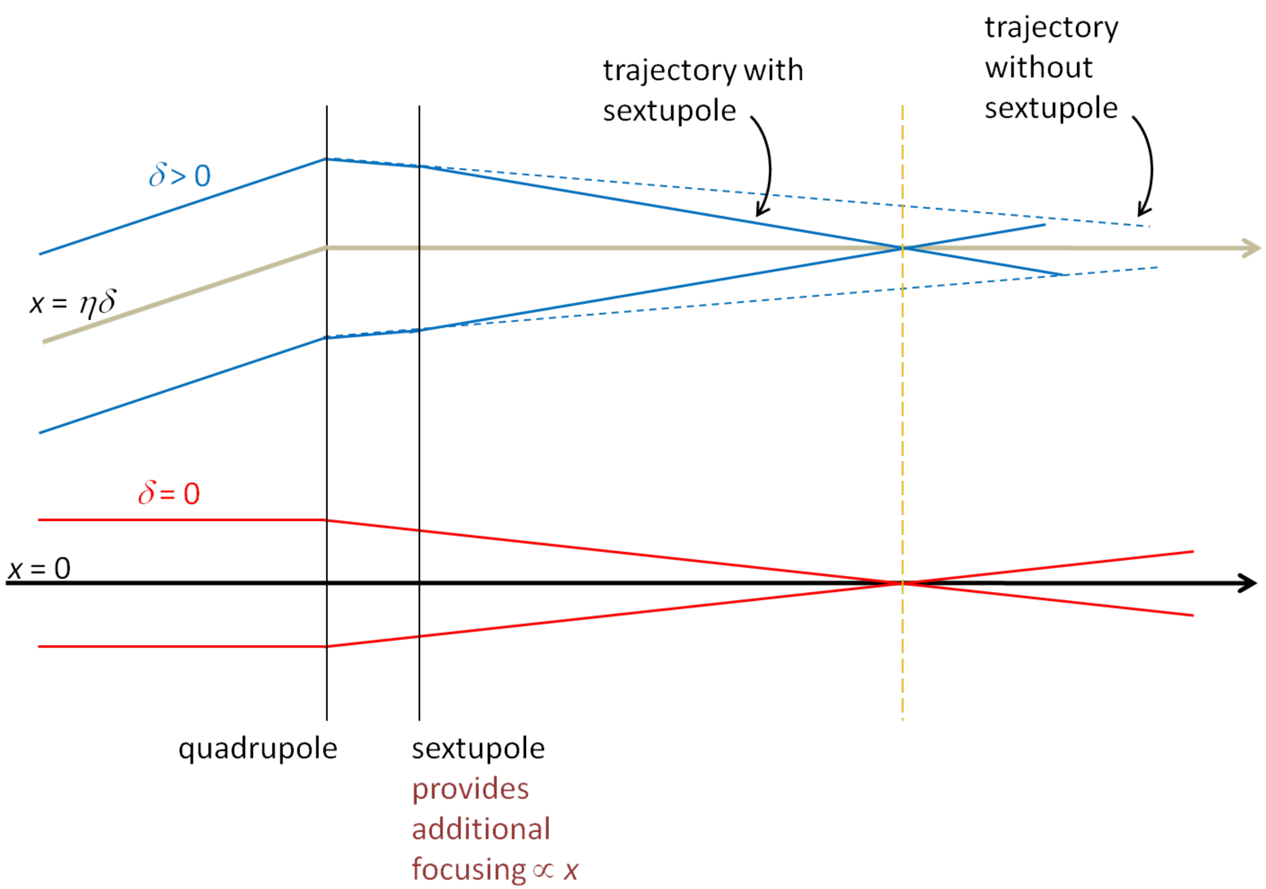

The chromaticity, and hence the sextupole strength, will normally be a function of the phase advance.

However, just to investigate the nonlinear effects of the sextupoles, we shall keep the sextupole strength $k_2L$ fixed, and change only the phase advance.

We can assume that the map from one sextupole to the next is linear, and corresponds to a rotation in phase space through an angle equal to the phase advance:

$$\begin{pmatrix} x \\ p_x \end{pmatrix} \mapsto \begin{pmatrix} \cos\mu_x & \sin\mu_x \\ -\sin\mu_x & \cos\mu_x \end{pmatrix} \begin{pmatrix} x \\ p_x \end{pmatrix}. \tag{1}$$

Again to keep things simple, we shall consider only horizontal motion, and assume that the vertical co-ordinate $y = 0$.

The change in the horizontal momentum of a particle moving through the sextupole is found by integrating the Lorentz force:

$$\Delta p_x = -\int_0^L \frac{B_y}{B\rho}\,ds. \tag{2}$$

The sextupole strength $k_2$ is defined by:

$$k_2 = \frac{1}{B\rho}\frac{\partial^2 B_y}{\partial x^2}, \tag{3}$$

where $B\rho$ is the beam rigidity. For a pure sextupole field (assuming that the vertical co-ordinate $y = 0$),

$$\frac{B_y}{B\rho} = \frac{1}{2}k_2 x^2. \tag{4}$$

If the sextupole is short, then we can neglect the small change in the co-ordinate $x$ as the particle moves through the sextupole, in which case:

$$\Delta p_x \approx -\frac{1}{2}k_2 L x^2. \tag{5}$$

The map for a particle moving through a short sextupole can be represented by a "kick" in the horizontal momentum:

$$x \mapsto x, \tag{6}$$

$$p_x \mapsto p_x - \frac{1}{2}k_2 L x^2. \tag{7}$$

Let us choose a fixed value $k_2 L = -600\,\mathrm{m}^{-2}$, and look at the effects of the maps for different phase advances.

For each case, we construct a *phase space portrait* by plotting the values of the dynamical variables after repeated application of the map (equation (1), followed by (6) and (7)) for a range of initial conditions.

First, let us look at the phase space portraits for a range of phase advances from $0.2 \times 2\pi$ to $0.5 \times 2\pi$.

# Phase space portraits: storage ring with a single sextupole

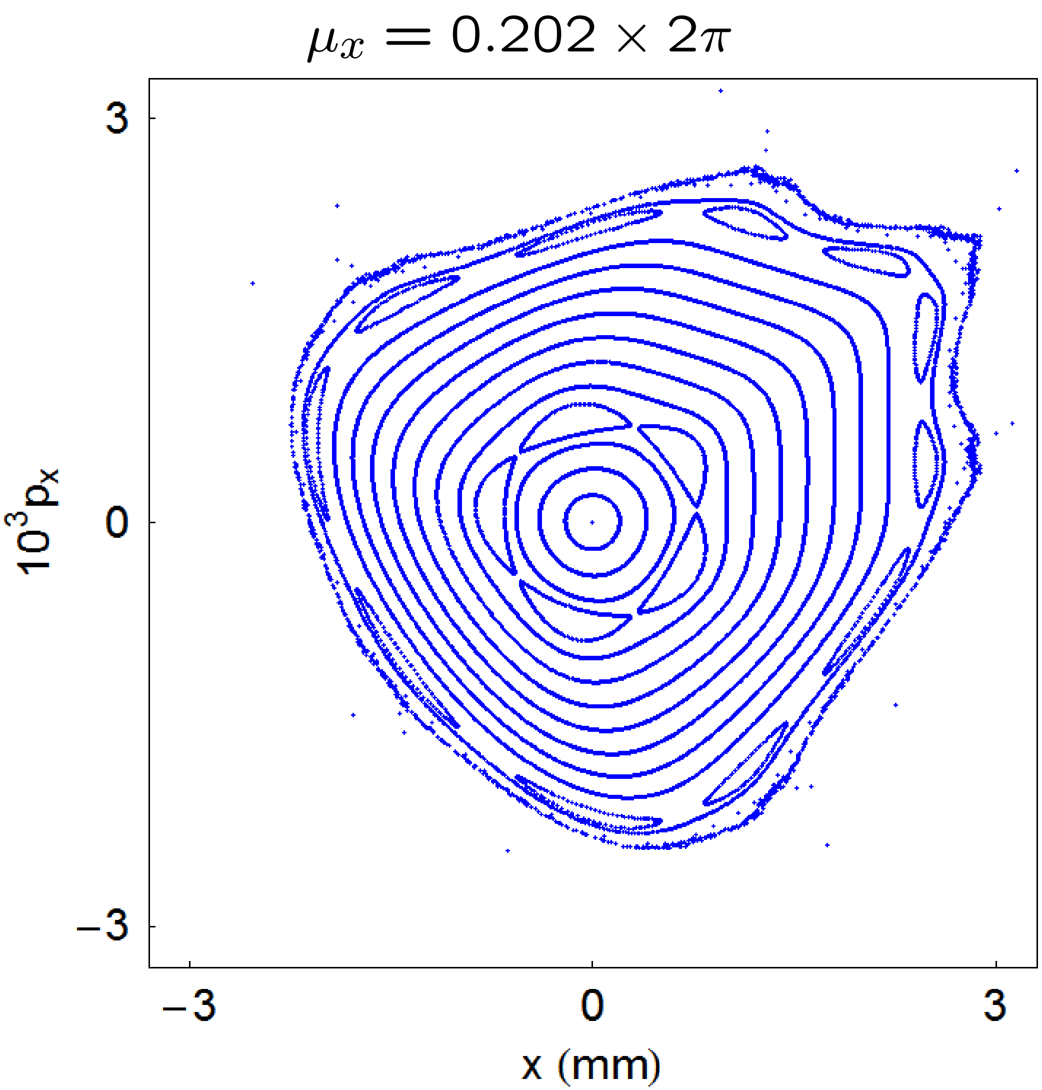

# Phase space portraits: storage ring with a single sextupole

$\mu_x = 0.252 \times 2\pi$

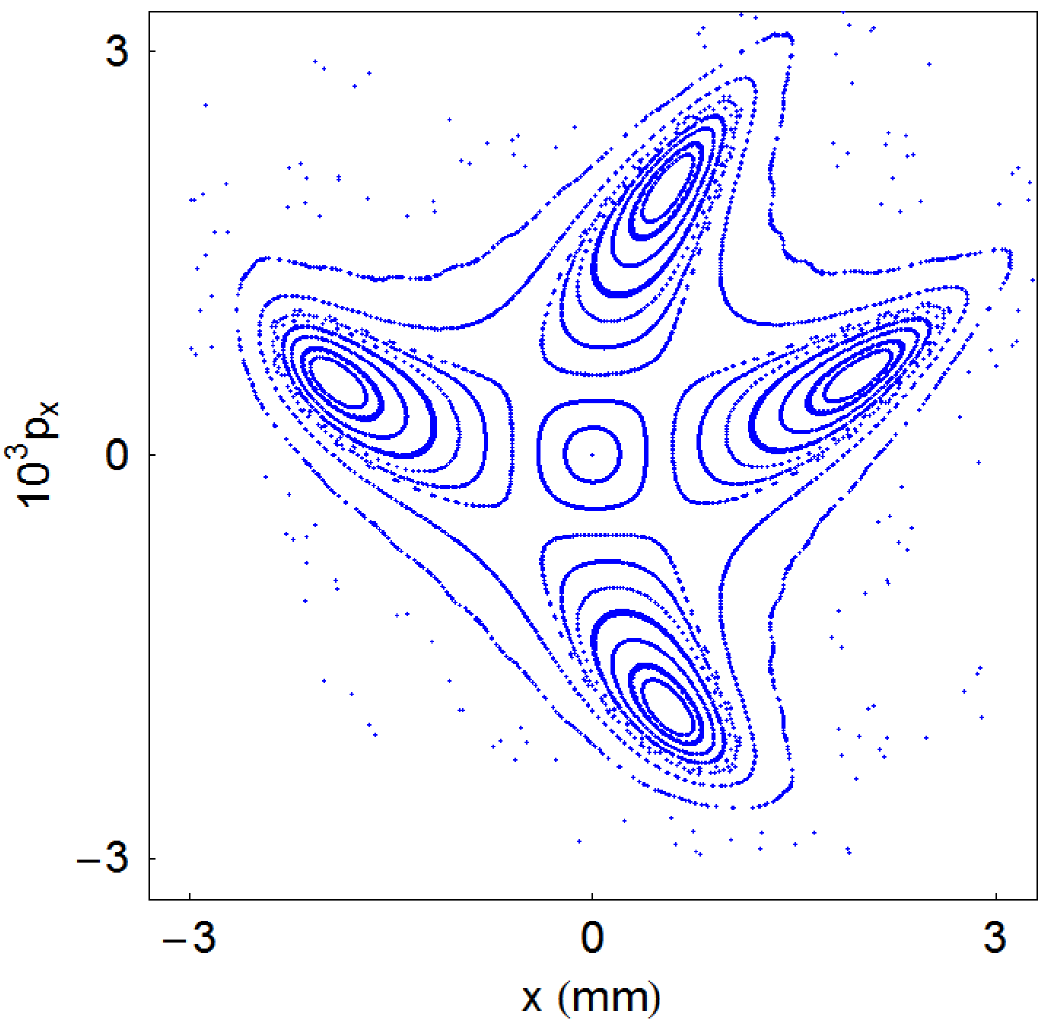

# Phase space portraits: storage ring with a single sextupole

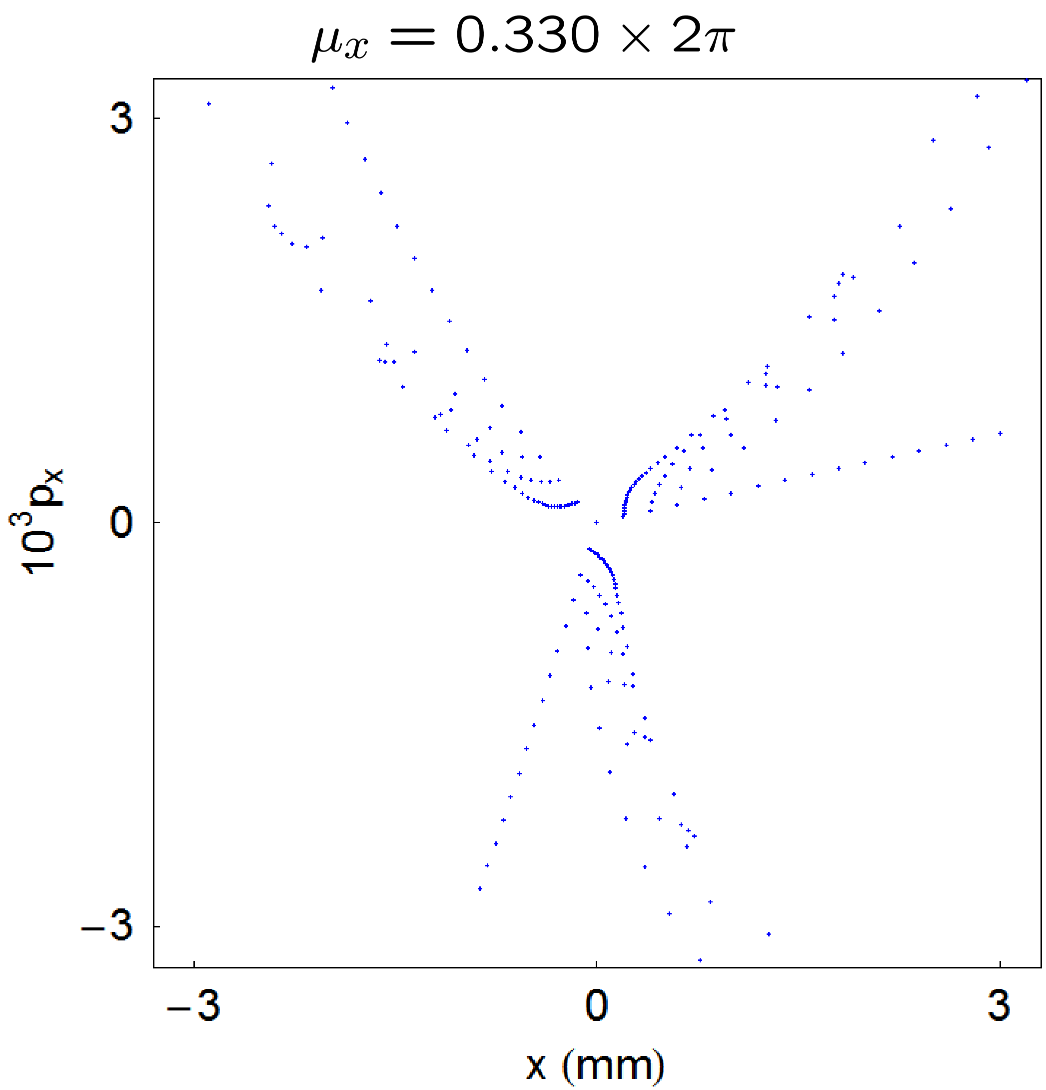

# Phase space portraits: storage ring with a single sextupole

$$\mu_x = 0.402 \times 2\pi$$

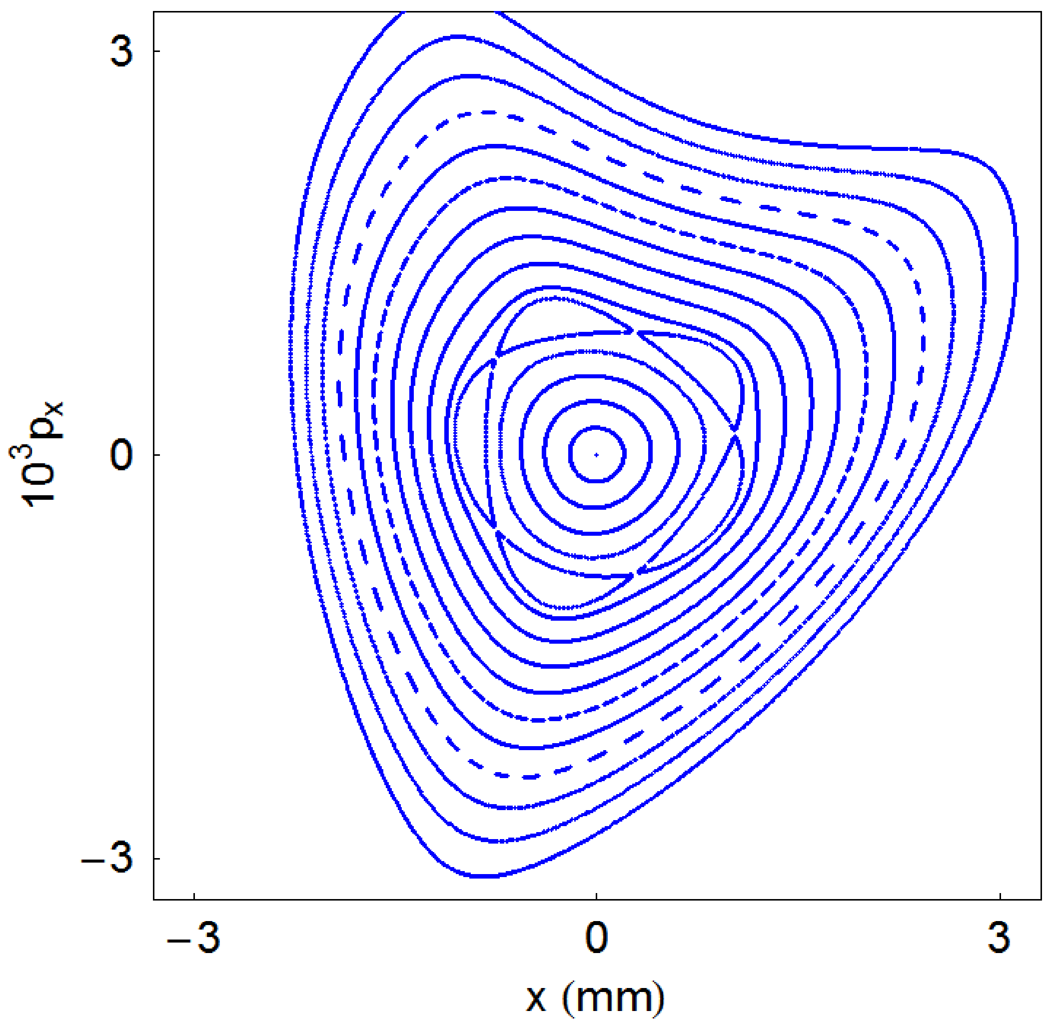

# Phase space portraits: storage ring with a single sextupole

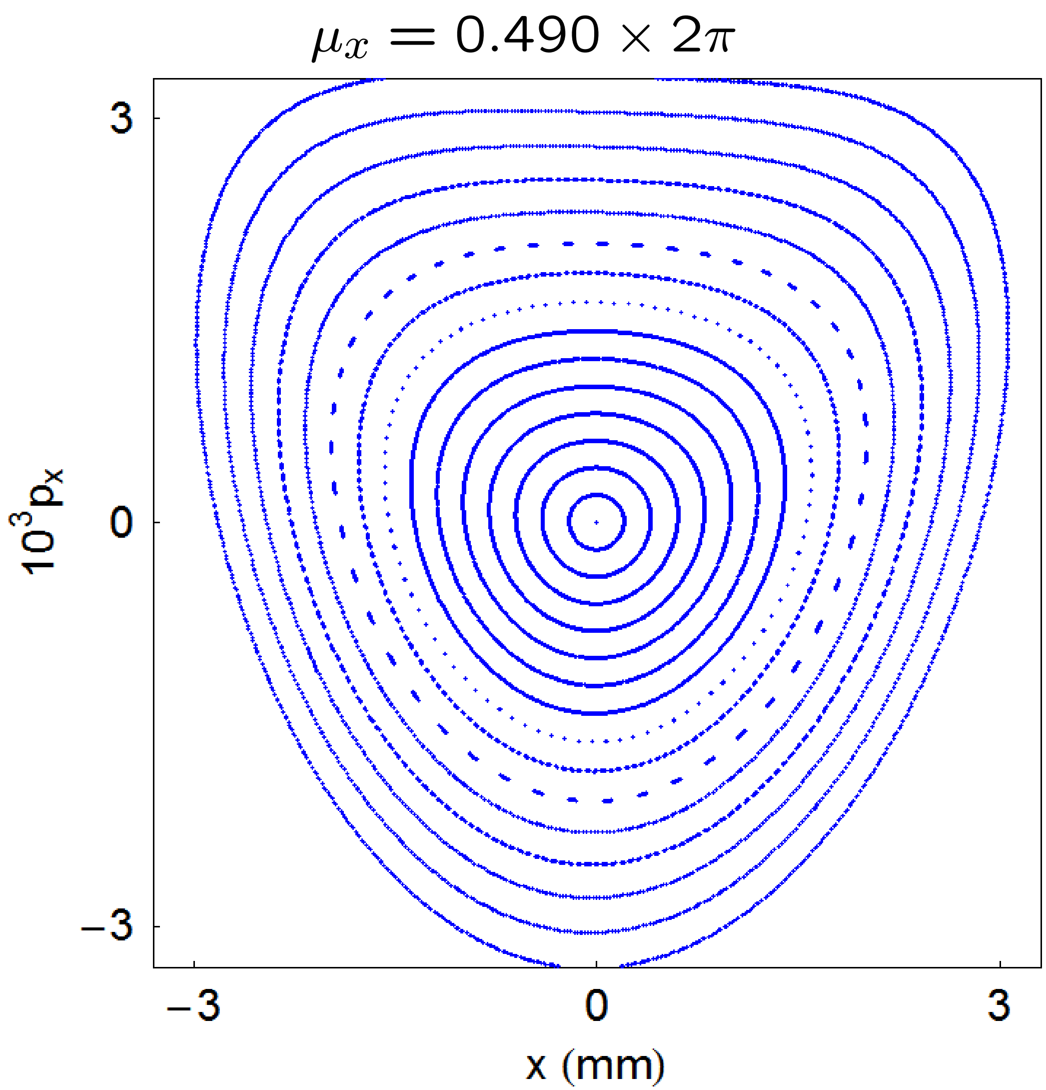

## Phase space portraits: storage ring with a single sextupole

There are some interesting features in these phase space portraits to which it is worth drawing attention:

- For small amplitudes (small $x$ and $p_x$), particles trace out closed loops around the origin: this is what we expect for a purely linear map.

- As the amplitude is increased, there appear "islands" in phase space: the phase advance (for the linear map) is often close to $m/p$ where $m$ is an integer and $p$ is the number of islands.

- Sometimes, a larger number of islands appears at larger amplitude.

- Usually, there is a closed curve that divides a region of stable motion from a region of unstable motion. Outside that curve, the amplitude of particles increases without limit as the map is repeatedly applied.

- The area of the stable region depends strongly on the phase advance: for a phase advance close to $2\pi/3$, it appears that the stable region almost vanishes altogether.

- It appears that as the phase advance is increased towards $\pi$, the stable area becomes large, and distortions from the linear ellipse become less evident.

An important observation is that the effect of the sextupole in the periodic cell depends strongly on the phase advance across the cell.

We can start to understand the significance of the phase advance by considering two special cases:

1. phase advance equal to an integer times $2\pi$;
2. phase advance equal to a half integer times $2\pi$.

Let us consider first what happens when the phase advance is an integer. In that case, the linear part of the map is just the identity:

$$x \mapsto x, \tag{8}$$

$$p_x \mapsto p_x. \tag{9}$$

So the combined effect of the linear map and the sextupole kick is:

$$x \mapsto x, \tag{10}$$

$$p_x \mapsto p_x - \frac{1}{2}k_2 L x^2. \tag{11}$$

Clearly, for $x \neq 0$, the horizontal momentum will increase without limit. There are no stable regions of phase space, apart from the line $x = 0$.

Now consider what happens if the phase advance of a cell is a half integer times $2\pi$, so the linear part of the map is just a rotation through $\pi$.

If a particle starts at the entrance of a sextupole with $x = x_0$ and $p_x = p_{x0}$, then at the exit of that sextupole:

$$x_1 = x_0, \tag{12}$$

$$p_{x1} = p_{x0} - \frac{1}{2} k_2 L x_0^2. \tag{13}$$

Then, after passing to the entrance of the next sextupole, the co-ordinates will be:

$$x_2 = -x_1 = -x_0, \tag{14}$$

$$p_{x2} = -p_{x1} = -p_{x0} + \frac{1}{2} k_2 L x_0^2. \tag{15}$$

Finally, on passing through the second sextupole:

$$x_3 = x_2 = -x_0, \tag{16}$$

$$p_{x3} = p_{x2} - \frac{1}{2}k_2 L x_2^2 = -p_{x0}. \tag{17}$$

In other words, the momentum kicks from the two sextupoles cancel each other exactly.

The resulting map is a purely linear phase space rotation by $\pi$.

In this situation, we expect the motion to be stable (and periodic), no matter what the amplitude.

The effect of the phase advance on the sextupole "kicks" is similar to the effect on perturbations arising from dipole and quadrupole errors in a storage ring.

In the case of dipole errors, the kicks add up if the phase advance is an integer, and cancel if the phase advance is a half integer.

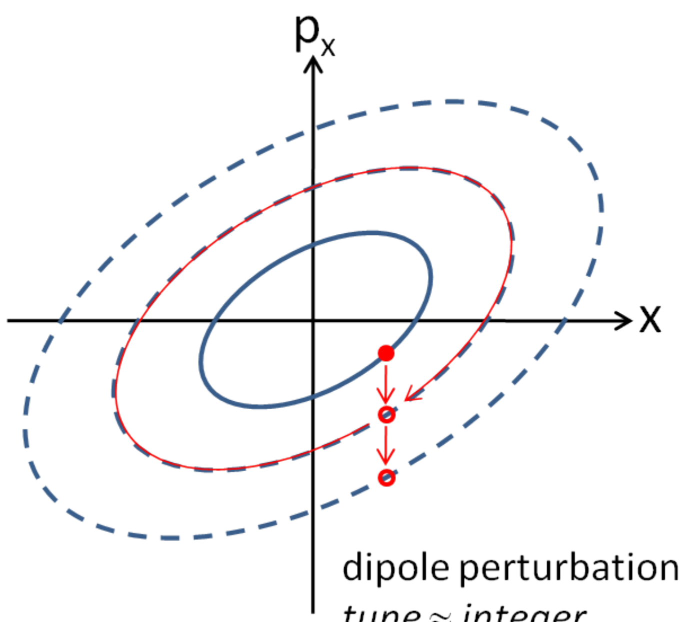


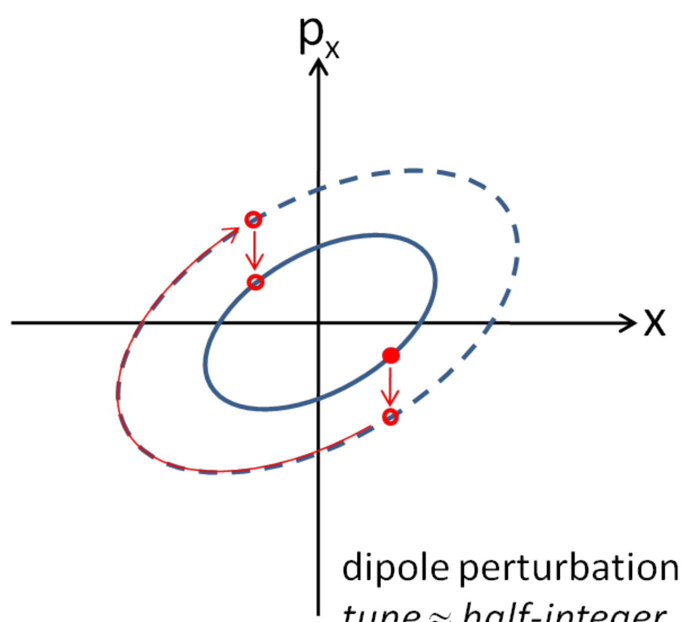

In the case of quadrupole errors, the kicks add up if the phase advance is a half integer.

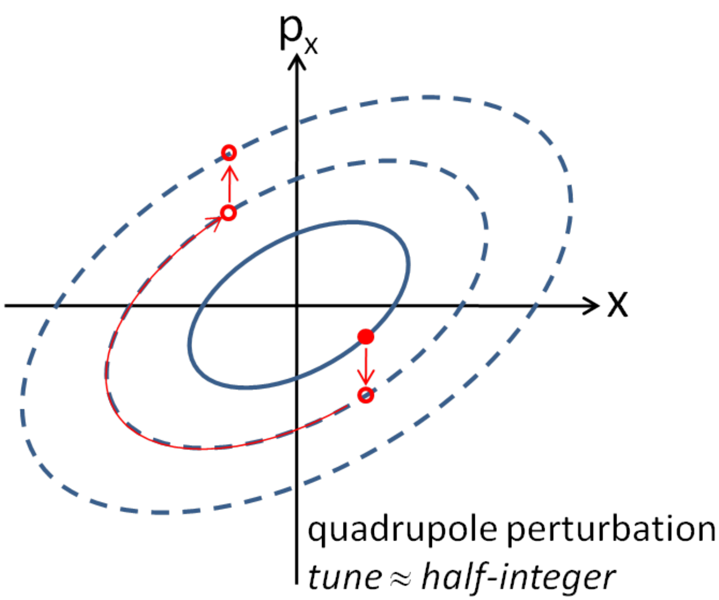


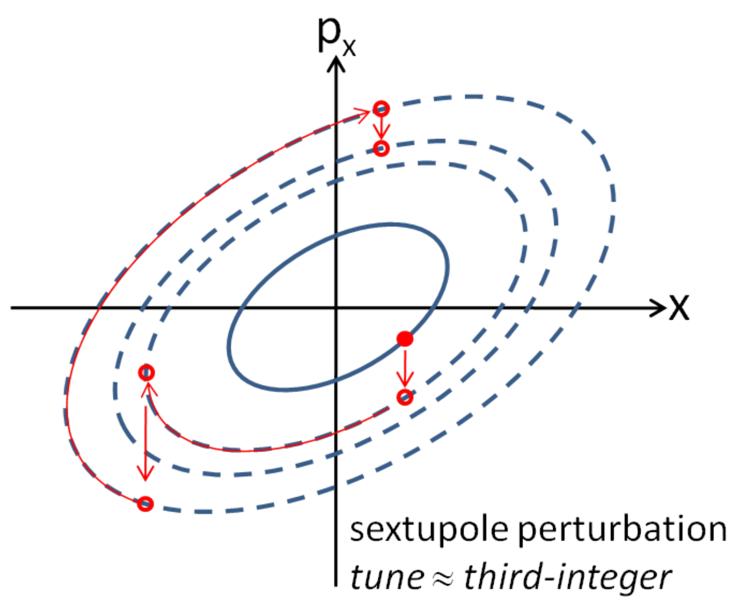


Higher-order multipoles drive higher-order resonances... but the effects are less easily illustrated on a phase space diagram.

If we include vertical as well as horizontal motion, then we find that resonances occur when the tunes satisfy:

$$m_x \nu_x + m_y \nu_y = \ell, \qquad (18)$$

where $m_x$, $m_y$ and $\ell$ are integers.

The order of the resonance is $|m_x| + |m_y|$.

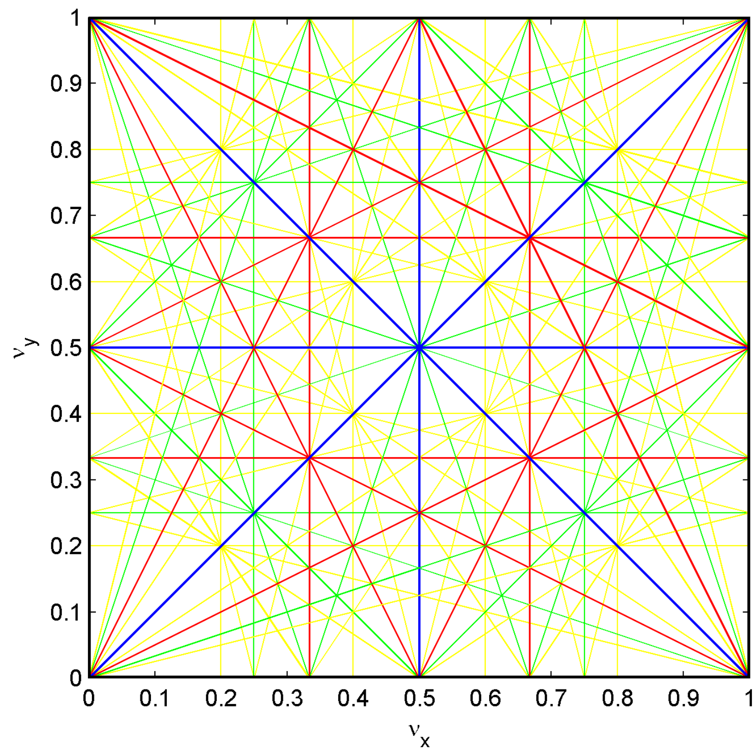

Resonances are associated with unstable motion for particles in storage rings.

However, the number of resonance lines in tune space is infinite: any point in tune space will be close to a resonance of some order.

This observation raises two questions:

1. How do we know what the real effect of any given resonance line will be?

2. How can we design a storage ring to minimise the adverse effects of resonances?

These are not easy questions to answer. We shall discuss some of the issues in the remaining parts of this lecture.

To begin with, for any analysis of nonlinear dynamics we need a convenient way to represent nonlinear transfer maps.

In our analysis of a bunch compressor, we represented the transfer maps for the rf cavity and the chicane as Taylor series.

For example, the longitudinal transfer map for the chicane is:

$$
\begin{aligned}
z_1 &= z_0 + 2L_1 \left( \frac{1}{\cos\theta_0} - \frac{1}{\cos\theta} \right), && (19) \\
\delta_1 &= \delta_0, && (20)
\end{aligned}
$$

where:

$$
\theta = \frac{\theta_0}{1+\delta_0}. \qquad (21)
$$

The map for a chicane can be expanded as a Taylor series:

$$z_1 = z_0 + R_{56}\delta_0 + T_{566}\delta_0^2 + U_{5666}\delta_0^3 + \ldots \quad (22)$$

$$\delta_1 = \delta_0, \quad (23)$$

where the coefficients $R_{56}$, $T_{566}$, $U_{5666}$ etc. are all functions of the chicane parameters $L_1$ and $\theta_0$.

Taylor series provide a convenient way of systematically representing transfer maps for beamline components, or sections of beamline.

The main drawback of Taylor series is that in general, transfer maps can only be represented exactly by series with an infinite number of terms.

In practice, we have to truncate a Taylor map at some order, and we then lose certain desirable properties of the map: in particular, a truncated map will not usually be *symplectic*.

Mathematically, a transfer map is symplectic if it satisfies the condition:

$$J^{\mathsf{T}} S J = S, \tag{24}$$

where $J_{mn} = \partial x_{m,f} / \partial x_{n,i}$ is the Jacobian of the map, and $S$ is the antisymmetric matrix with block diagonals:

$$S_2 = \begin{pmatrix} 0 & 1 \\ -1 & 0 \end{pmatrix}. \tag{25}$$

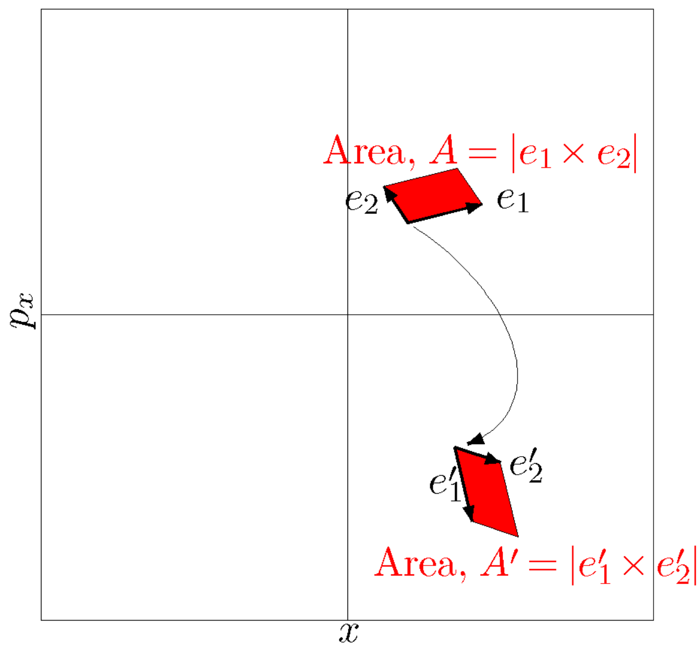


Physically, a symplectic transfer map conserves phase space volumes when the map is applied.

This is Liouville's theorem, and is a property of charged particles moving in electromagnetic fields, in the absence of radiation.

The effect of losing symplecticity becomes apparent if we compare phase space portraits constructed using symplectic (below, left) and non-symplectic (below, right) transfer maps.

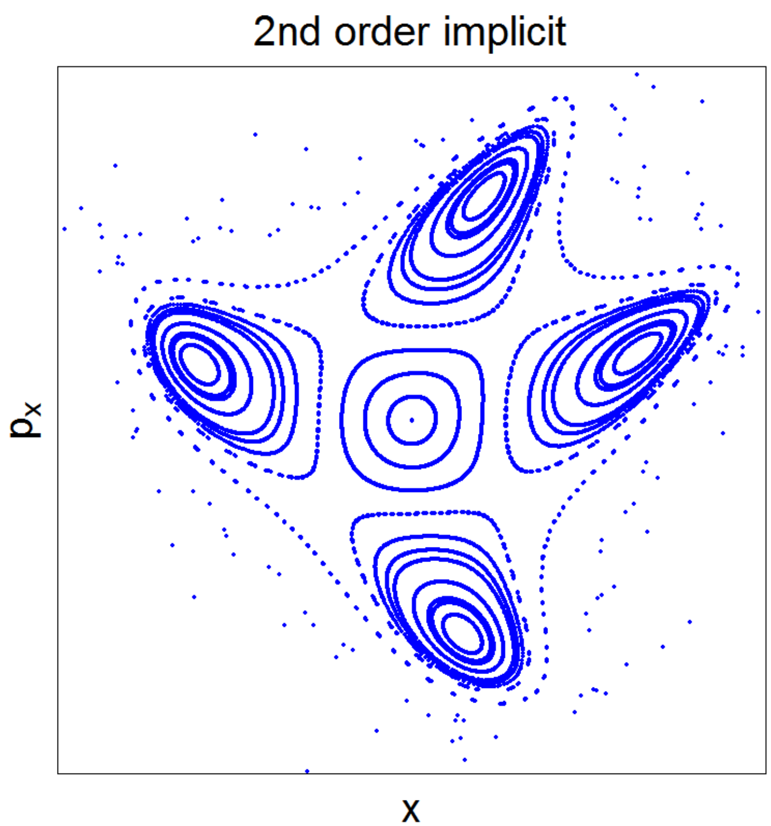


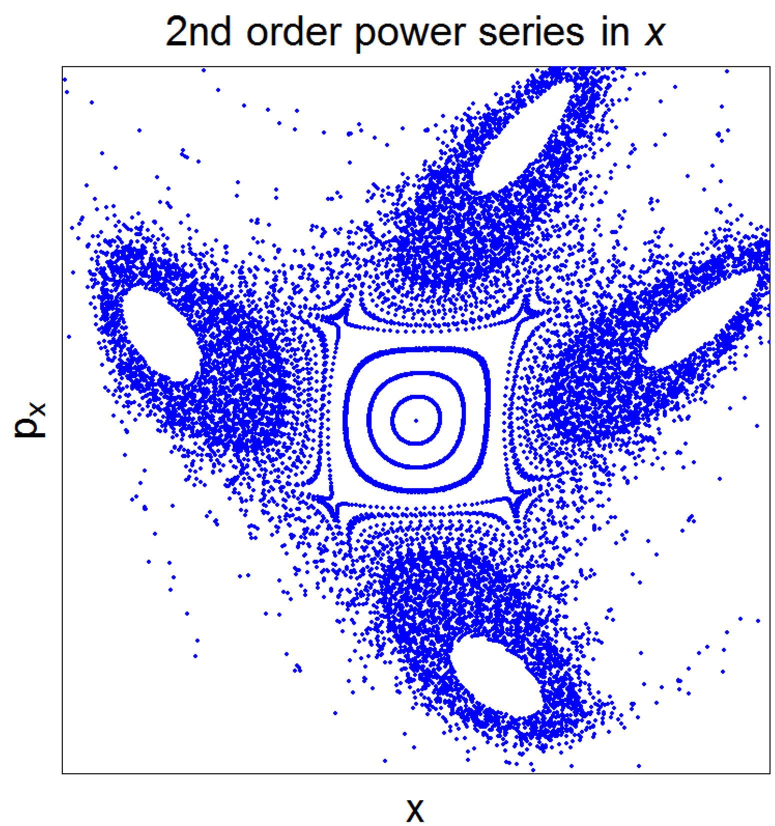

There are a number of ways of representing transfer maps to ensure symplecticity. These include:

- Taylor maps can be specially constructed to retain symplecticity with a certain (finite) number of terms. Taylor maps are *explicit*: once the coefficients have been calculated, the map can be applied simply by substitution of values for the dynamical variables.

- Mixed-variable generating functions provide an *implicit* representation: each application of the map requires further solution of equations (see Appendix B).

- Lie transformations provide a finite representation for infinite Taylor series, and are useful for analytical studies (see Appendix C).

Symplectic Taylor maps with a finite number of terms can be constructed for multipole magnets of any order using the "kick" approximation.

As an example, consider a sextupole, for which the (approximate) equations of motion are:

$$\frac{dx}{ds} = p_x, \qquad \frac{dp_x}{ds} = -\frac{1}{2}k_2 x^2. \tag{26}$$

These equations do not have an exact solution in terms of elementary functions.

However, by splitting the integration into three steps it is possible to write down an approximate solution that is explicit and symplectic:

$$0 \le s < L/2: \qquad x_1 = x_0 + p_{x0}, \quad p_{x1} = p_{x0}, \tag{27}$$

$$s = L/2: \qquad x_2 = x_1, \quad p_{x2} = p_{x1} - \frac{1}{2}k_2 L x_1^2, \tag{28}$$

$$L/2 < s \le L: \qquad x_3 = x_2 + p_{x2}, \quad p_{x3} = p_{x2}. \tag{29}$$

The solution (27)–(28) is an example of a *symplectic integrator*. For obvious reasons, this particular integrator is known as a "drift–kick–drift" approximation.

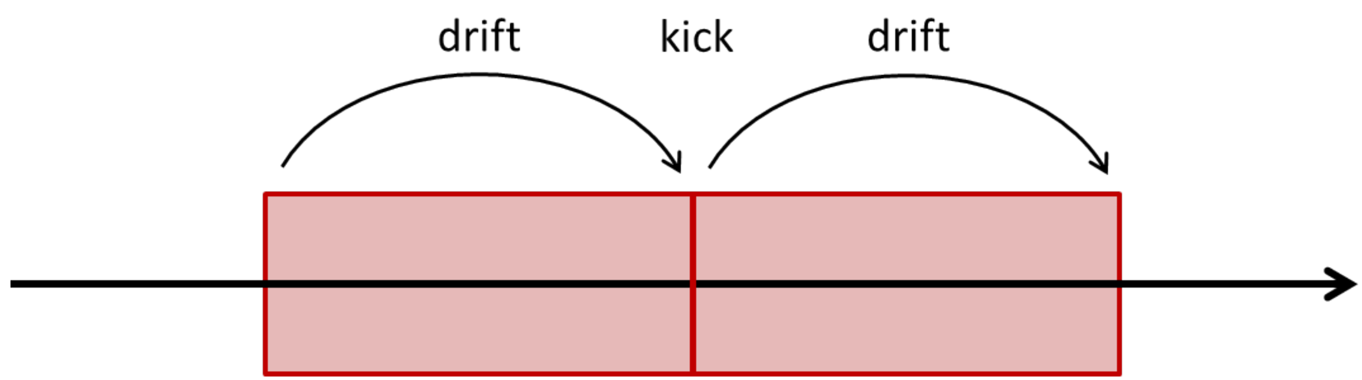


By splitting the integration into smaller steps, it is possible to obtain better approximations.

Using special techniques (e.g. from classical mechanics) it can be shown that by splitting a multipole in particular ways, it is possible to minimise the error for a given number of integration steps.

Taylor maps are useful for particle tracking, but do not give much insight into the dynamics of a given nonlinear system.

To develop a deeper understanding (e.g. to determine the impact of individual resonances) more powerful techniques are needed.

There are two approaches that are quite widely used in accelerator physics:

- perturbation theory;
- normal form analysis.

In both these techniques, the goal is to construct a quantity that is invariant under application of the single-turn transfer map. Unfortunately, in both cases the mathematics is complicated and fairly cumbersome.

In the case of a single sextupole in a storage ring, we find from normal form analysis the following expression for the betatron action $J_x$ as a function of the betatron phase (angle variable):

$$J_x \approx I_0 - \frac{k_2 L}{8}(2\beta_x I_0)^{3/2}\frac{(\cos(3\mu_x/2 + 2\phi_x) + \cos(\mu_x/2))}{\sin(3\mu_x/2)} + O(I_0^2),$$

where $I_0$ is a constant (an invariant of the motion), $\phi_x$ is the angle variable, and $\mu_x$ is the phase advance per cell.

Note that the second term in the expression for $J_x$ becomes very large when $\mu_x$ is close to a third integer.

The cartesian variables can be expressed in terms of the action–angle variables:

$$x = \sqrt{2\beta_x J_x}\cos\phi_x, \quad (30)$$

$$p_x = -\sqrt{\frac{2J_x}{\beta_x}}(\sin\phi_x + \alpha_x \cos\phi_x). \quad (31)$$

phase advance $\mu_x = 0.28 \times 2\pi$

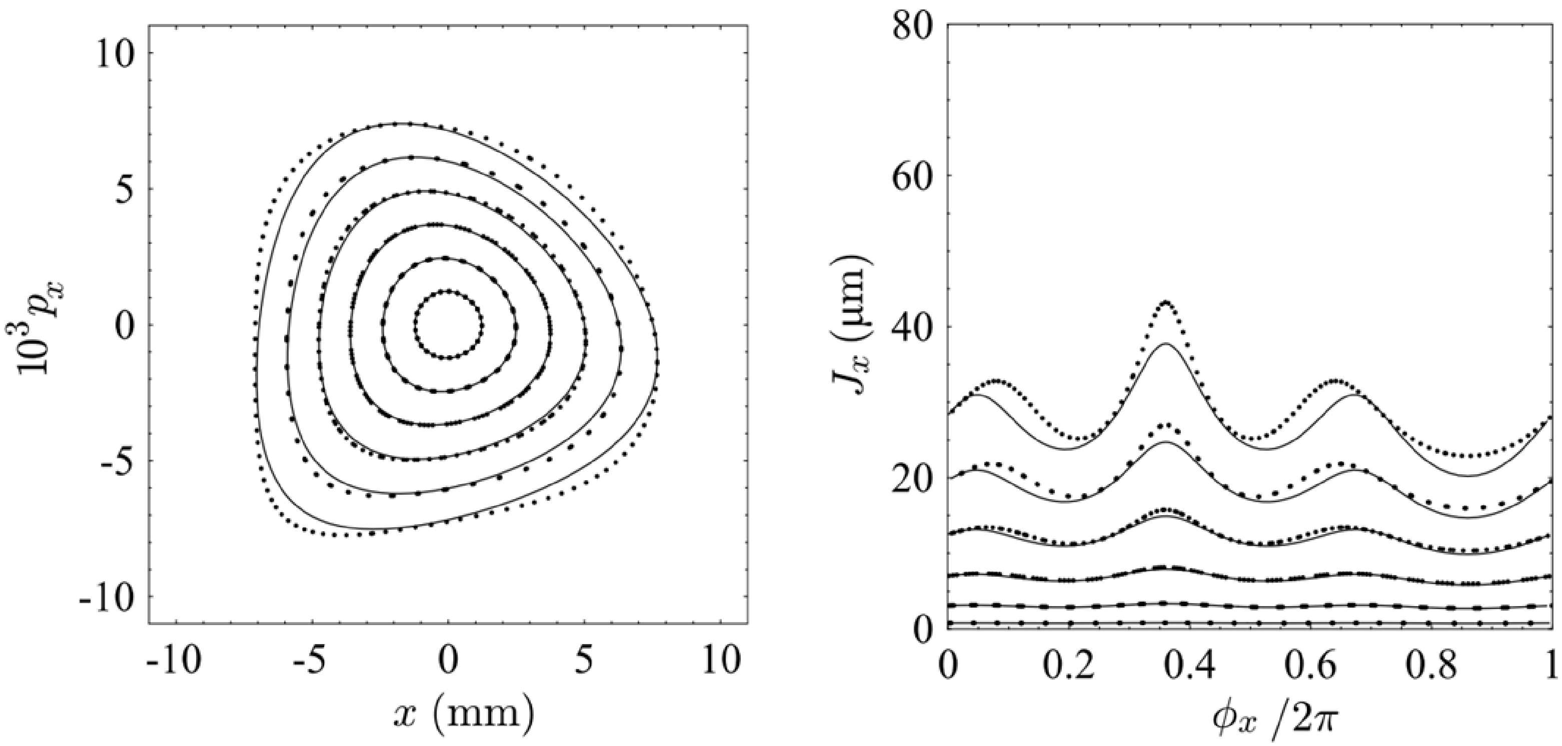

phase advance $\mu_x = 0.30 \times 2\pi$

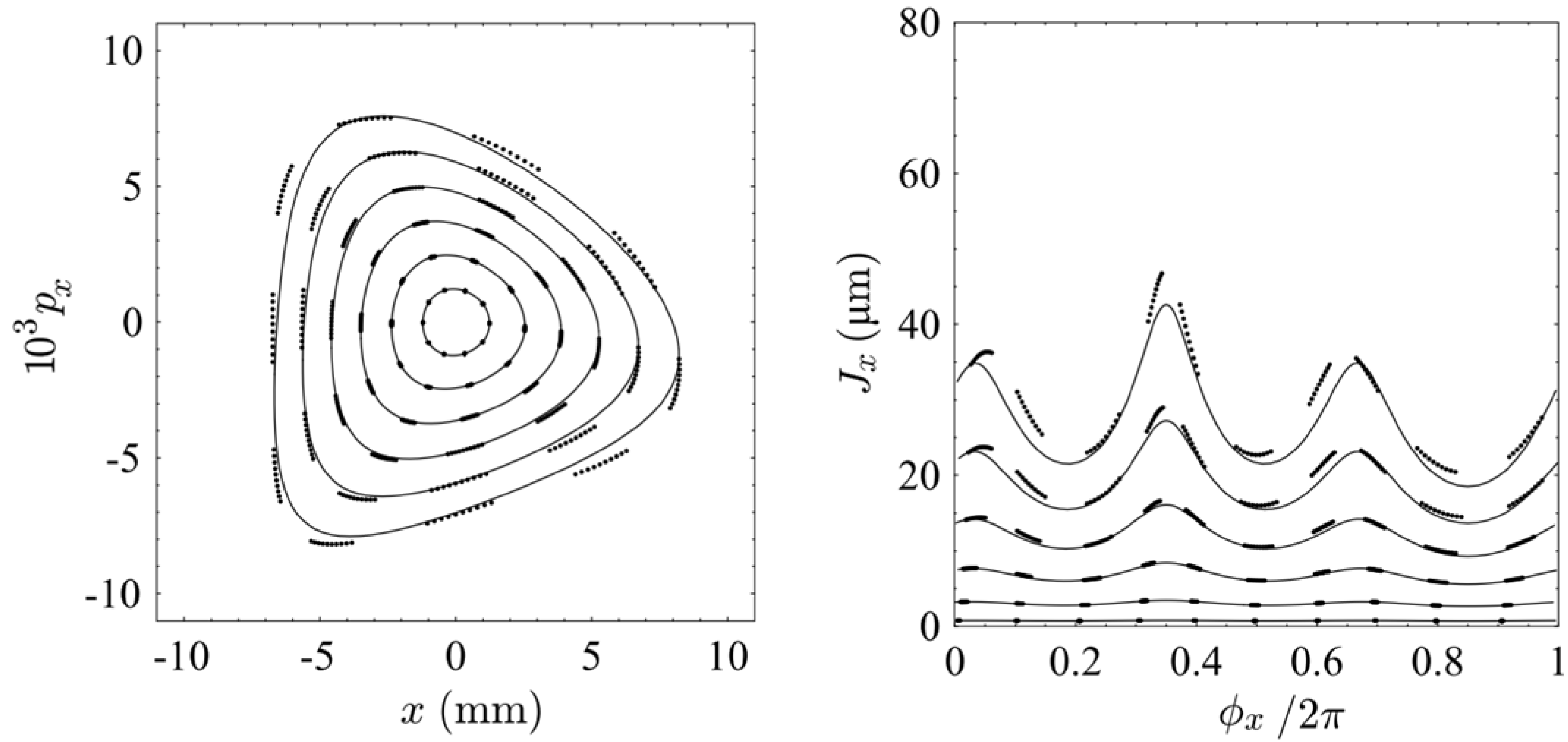

phase advance $\mu_x = 0.315 \times 2\pi$

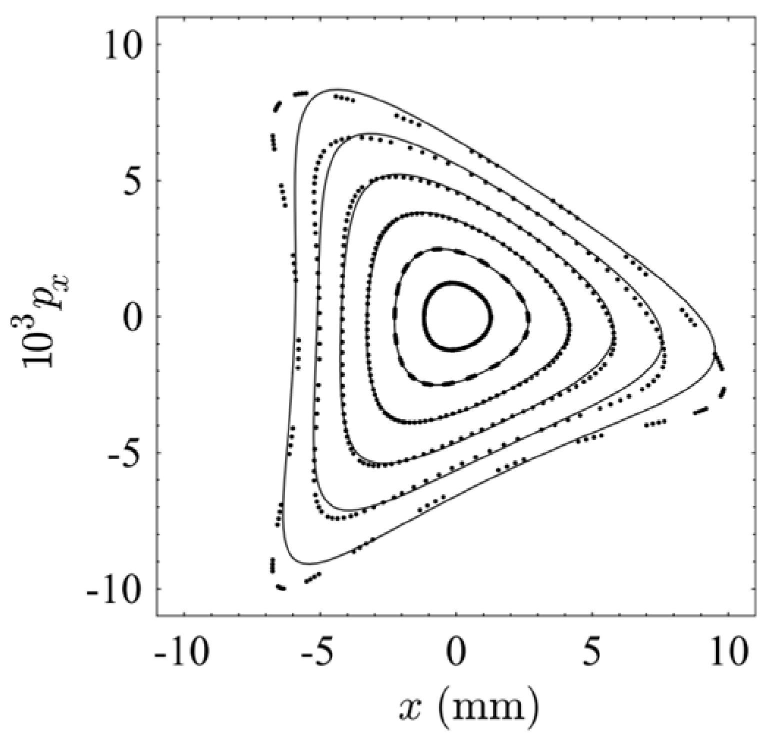


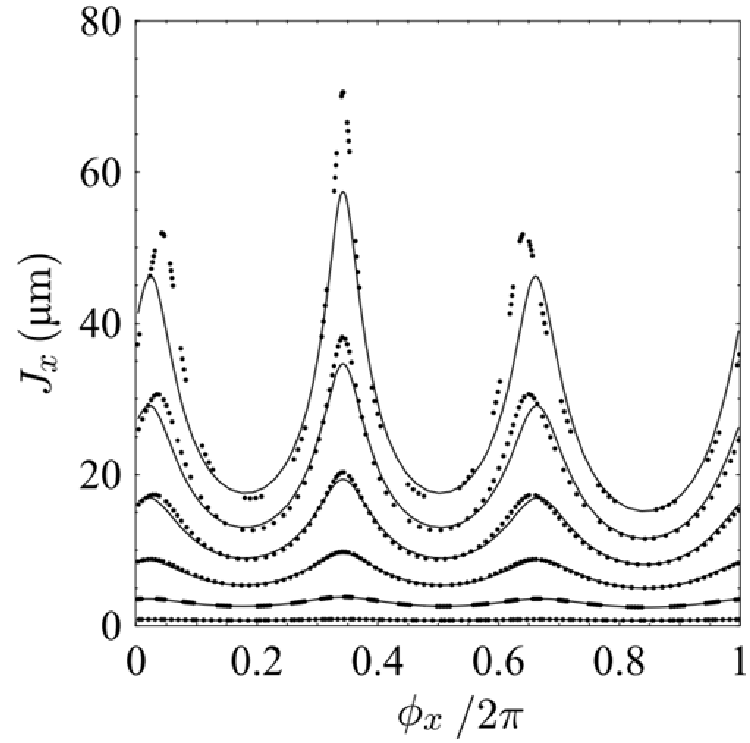

Close inspection of the plots on the previous slides reveals another effect, in addition to the obvious distortion of the phase space ellipses: the phase advance per turn (i.e. the tune) varies with increasing betatron amplitude.

Normal form analysis (and perturbation theory) can be used to obtain estimates for the tune shift with amplitude. In the case of a sextupole, the tune shift is higher-order in the action.

An octupole, however, does have a first-order (in the action) tune shift with amplitude, given by:

$$\nu_x = \nu_{x0} + \frac{k_3 L \beta_x^2}{16\pi} J_x + O(J_x^2). \tag{32}$$

The tune shift with amplitude becomes obvious if we track a small number of turns (30) in a lattice with a single octupole.

$\mu_x = 0.330 \times 2\pi$ $\mu_x = 0.336 \times 2\pi$

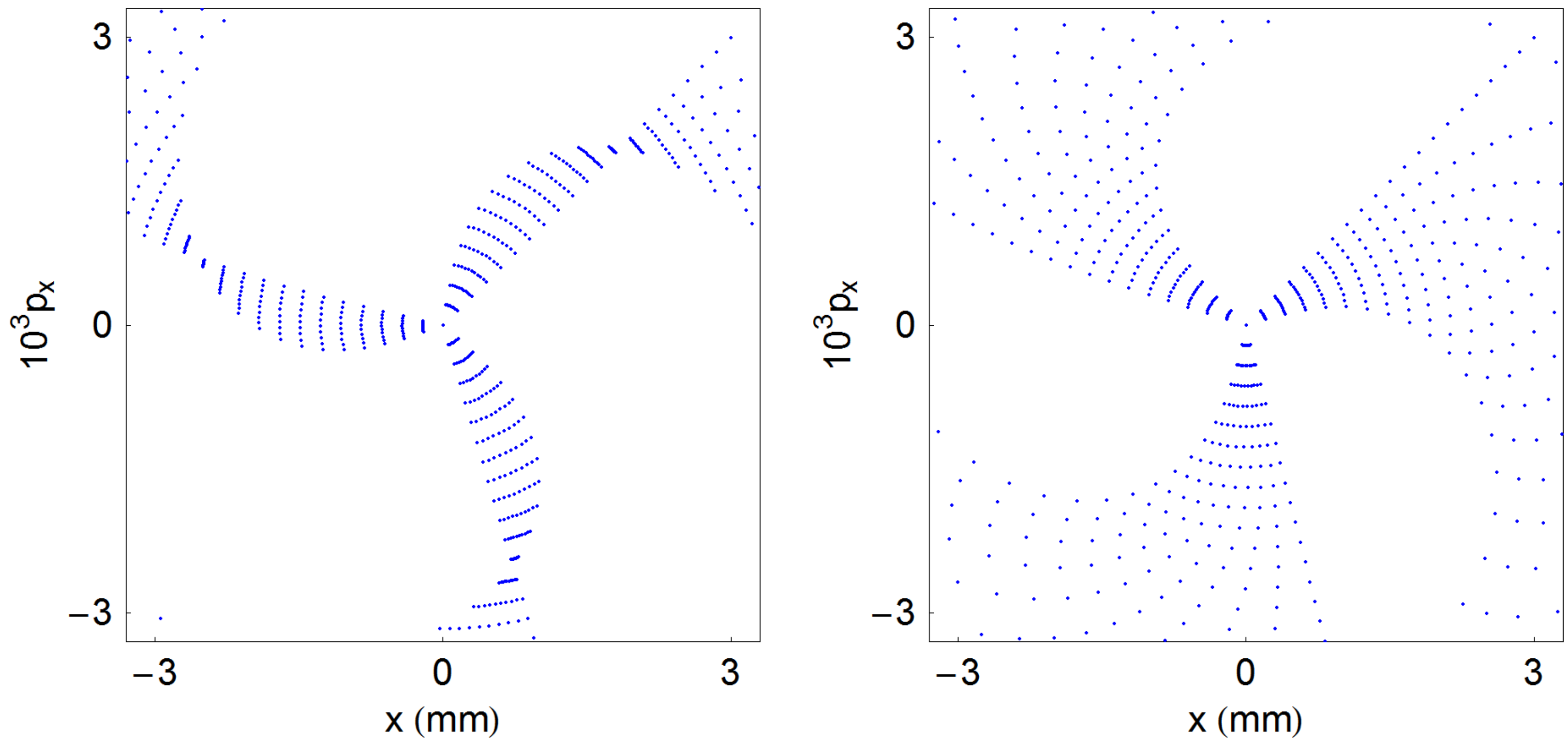

"Islands" appear in phase space portraits at amplitudes where the phase advance is $2\pi\times$ a rational number (that determines the number of islands), and where the transfer map contains a "driving term" (that determines the widths of the islands).

Recall the phase space portraits for a sextupole in a storage ring:

$\mu_x = 0.252 \times 2\pi$

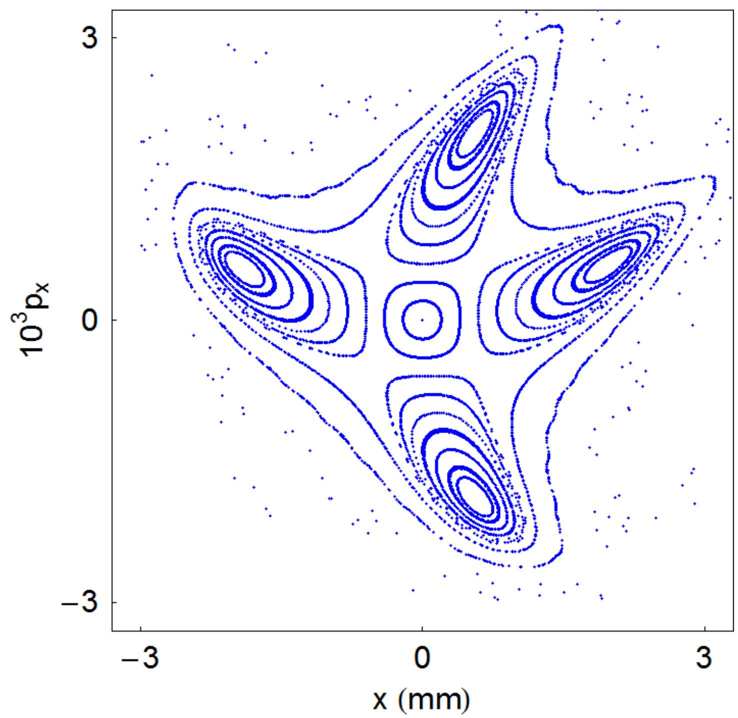


$\mu_x = 0.402 \times 2\pi$

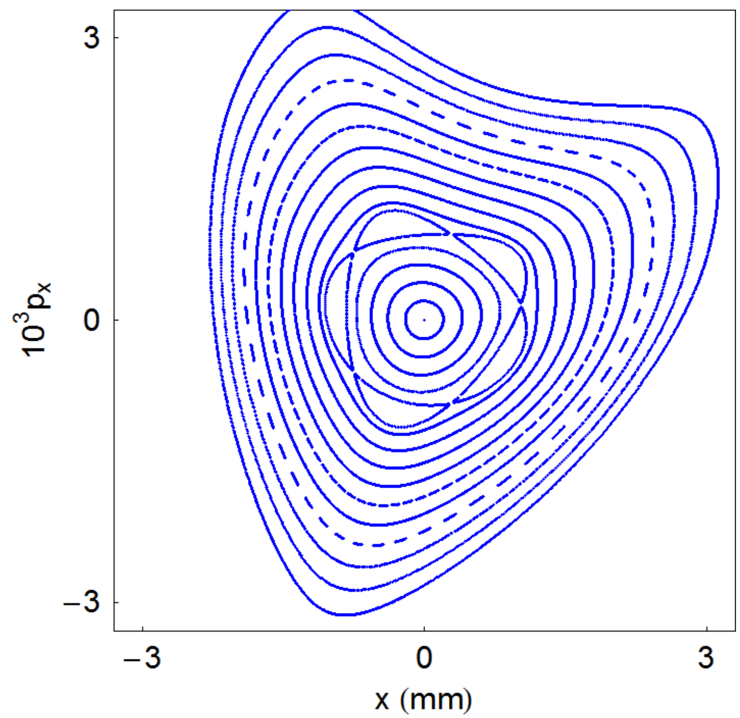

Perturbation theory and normal form analysis depend on the existence of constants of motion in the presence of nonlinear perturbations.

The fact that constants of motion can exist in the presence of nonlinear perturbations is a consequence of the Kolmogorov–Arnold–Moser (KAM) theorem.

The KAM theorem expresses the general conditions for the existence of constants of motion in nonlinear Hamiltonian systems.

Resonances do not invariably result in immediate loss of stability.

In particular, if the tune shift with amplitude is sufficiently large, then it is possible for there to be a stable region at amplitudes significantly larger than that at which resonance occurs.

However, the overlapping of two resonances is associated with a transition from regular to chaotic motion: the parameter range over which the particle motion becomes chaotic is described by the *Chirikov criterion*.

We have shown phase space portraits for motion in one degree of freedom. In those cases, instability occurred when the oscillation amplitude exceeded a certain value.

In multiple degrees of freedom, a new phenomenon occurs: *Arnold diffusion*. There can be regions of phase space where invariant tori exist at large amplitudes compared to regions of chaotic motion.

For storage rings, this means that trajectories with (initially) small amplitudes can be unstable, even if trajectories with much larger amplitudes are stable.

Frequency map analysis (FMA) applies "numerical analysis of the Fourier frequencies" to determine the tunes to high precision from tracking data.

The strengths of different resonances can be seen by plotting points in tune space, with diffusion rates shown by different colours.

The boundary of the stable region in co-ordinate space is known as the "dynamic aperture".

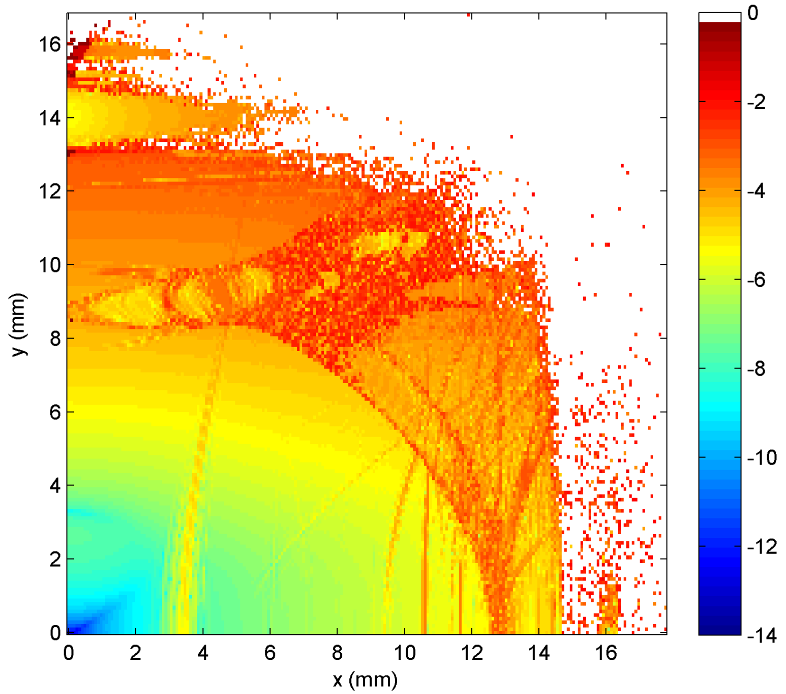


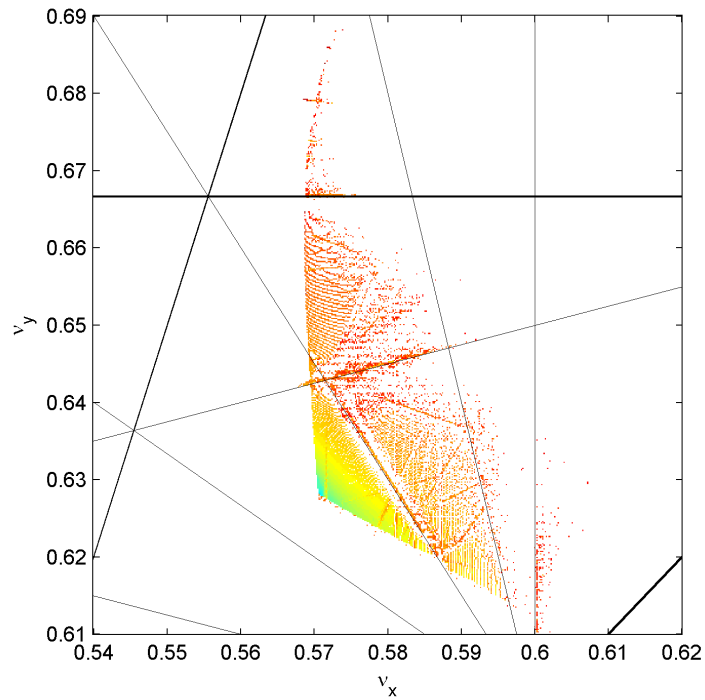


*FMA of CesrTA (J. Shanks, Cornell University).*

http://www.lepp.cornell.edu/~shanksj/research/20100629/2048_1024.html

A large dynamic aperture is needed for good injection efficiency, and good lifetime. The dynamic aperture shrinks with energy deviation, limiting the energy acceptance. In low-emittance electron storage rings, beam lifetime is often limited by the dynamic energy acceptance.

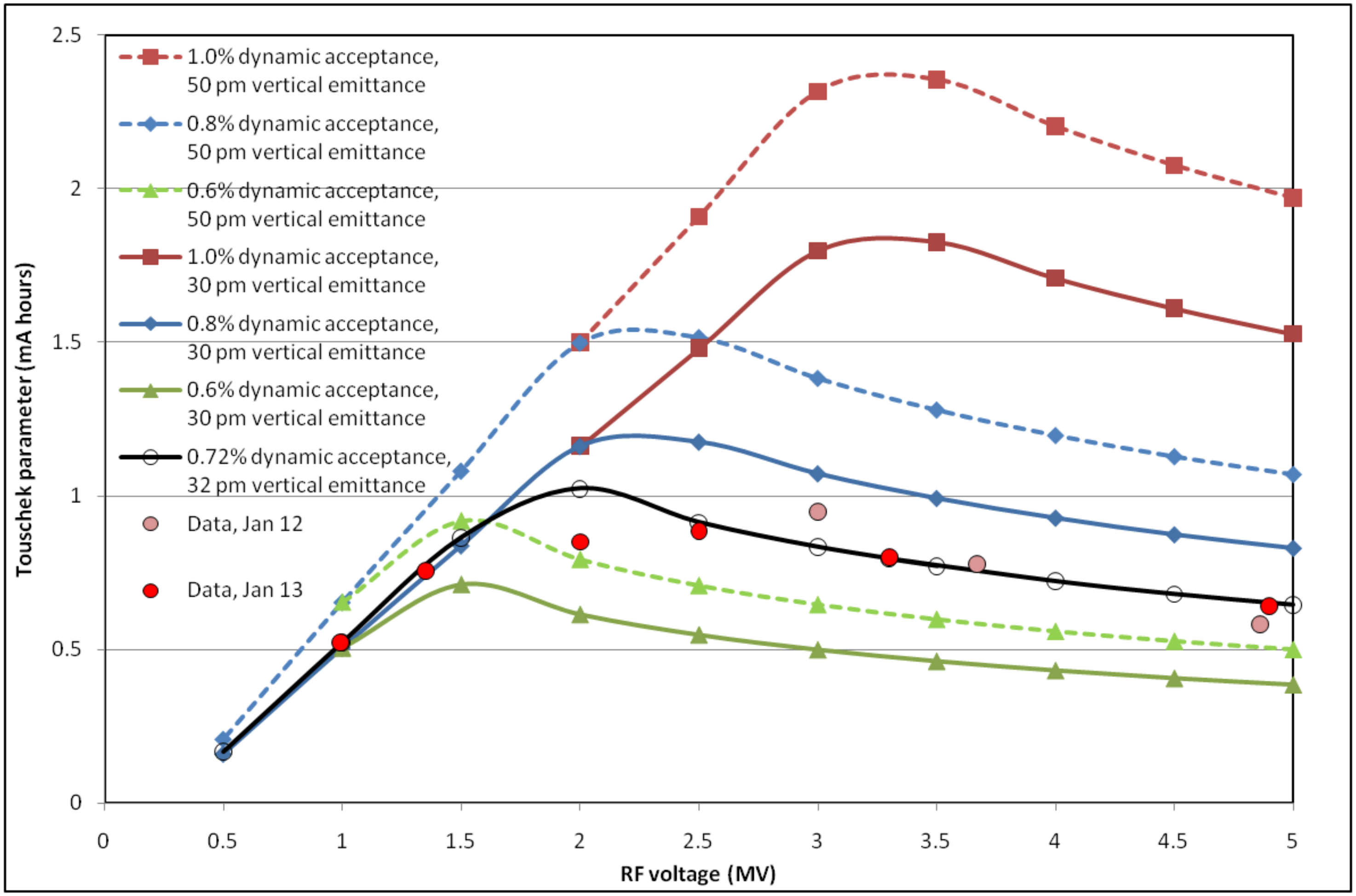

# Observation of resonance "islands" in the ALS

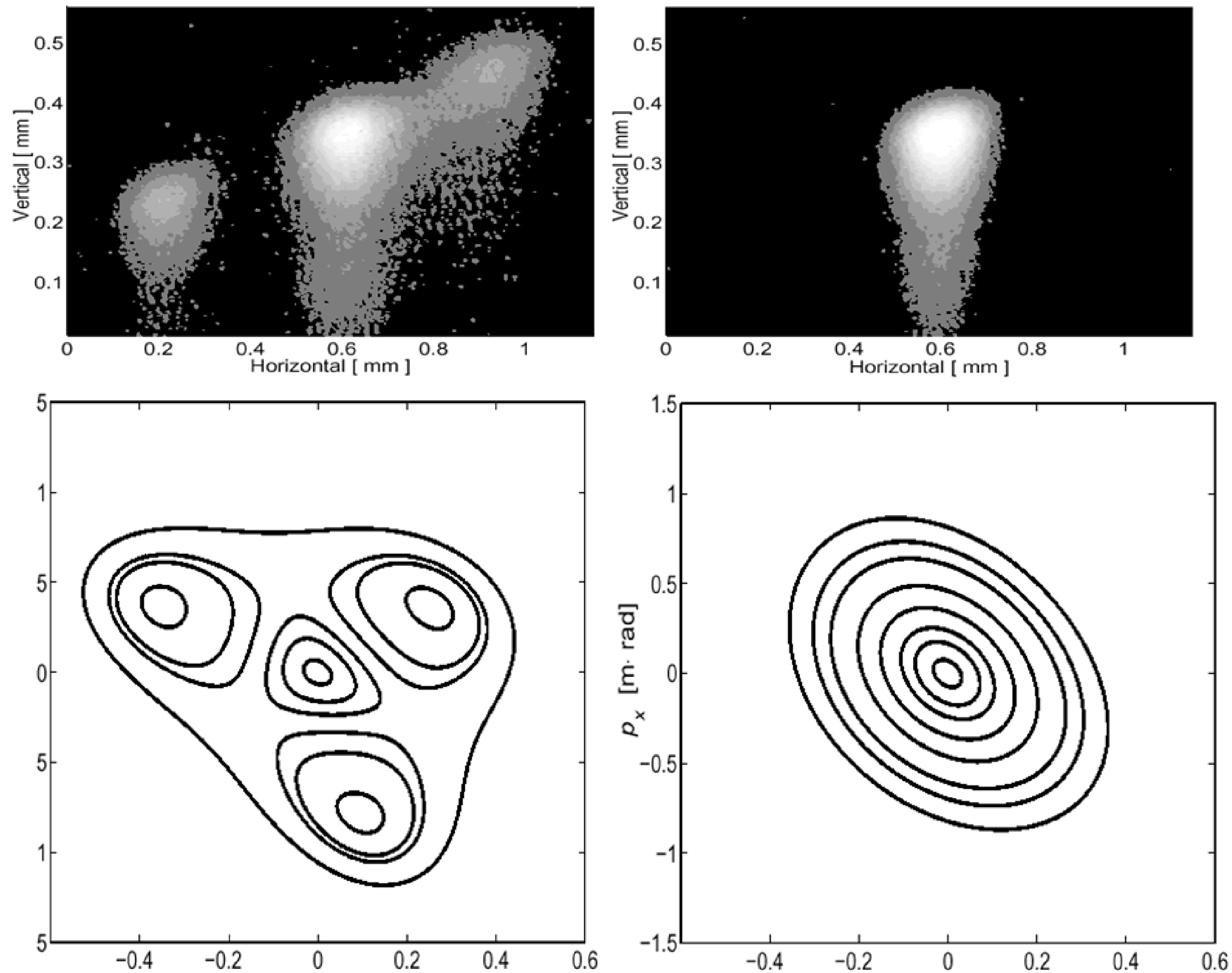


*D. Robin, C. Steier, J. Safranek, W. Decking, "Enhanced performance of the ALS through periodicity restoration of the lattice," proc. EPAC 2000.*

## Summary (1)

Nonlinear dynamics appear in a wide variety of accelerator systems, including single-pass systems (such as bunch compressors) and multi-turn systems (such as storage rings).

It is possible to model nonlinear dynamics in a given component or section of beamline by representing the transfer map as a power series.

A power series provides a convenient (explicit) representation of a transfer map for modelling and simple analysis of nonlinear dynamics in accelerators.

Conservation of phase space volumes is an important feature of the beam dynamics in many systems. To conserve phase space volumes, transfer maps must be symplectic.

In general, (truncated) power series maps are not symplectic. There are alternative representations that guarantee symplecticity, but are less convenient (e.g. because they are implicit).

To construct a symplectic transfer map, the equations of motion in a given accelerator component must be solved using a symplectic integrator (e.g. the "drift–kick–drift" approximation for a multipole magnet).

# Summary (3)

Common features of nonlinear dynamics in accelerators include phase space distortion, tune shifts with amplitude, resonances, and instability of particle trajectories at large amplitudes (dynamic aperture limits).

Analytical methods such as perturbation theory and normal form analysis can be used to estimate the impact of nonlinear perturbations in terms of quantities such as resonance strengths and tune shifts with amplitude.

Frequency map analysis provides a useful numerical tool for characterising tune shifts and resonance strengths from tracking data. This can give some insight into limitations on the dynamic aperture.

# Further reading

H. Goldstein, C.P. Poole Jr., J.L. Safko, *Classical Mechanics* (Pearson, 3rd edition, 2013).

H. Wiedemann, *Particle Accelerator Physics* (Springer, 3rd edition, 2007).

É. Forest, *Beam Dynamics: A New Attitude and Framework* (CRC Press, 1998).

É. Forest, *Geometric integration for particle accelerators*, Journal of Physics A: Mathematical and Theoretical 39, pp. 5321–5377 (2006).

A. Wolski, *Beam Dynamics in High Energy Particle Accelerators* (Imperial College Press, 2014).

Y. Papaphilippou, *Detecting chaos in particle accelerators through the frequency map analysis method*, Chaos: An Interdisciplinary Journal of Nonlinear Science 24, 024412 (2014). doi: 10.1063/1.4884495

# Appendices

A mixed-variable generating function represents a transfer map (or, more generally, a canonical transformation) in the form of a function of initial and final values of the phase space variables.

There are different kinds of generating function. A mixed-variable generating function of the third kind is expressed as a function of the initial momenta $\vec{p}$ and final co-ordinates $\vec{X}$:

$$F_3 = F_3(\vec{X}, \vec{p}). \tag{33}$$

The final momenta $\vec{P}$ and initial co-ordinates $\vec{x}$ are obtained by:

$$\vec{x} = -\frac{\partial F_3}{\partial \vec{p}}, \quad \text{and} \quad \vec{P} = -\frac{\partial F_3}{\partial \vec{X}}. \tag{34}$$

As an example, consider the mixed-variable generating function in one degree of freedom:

$$F_3 = -X p_x + \frac{1}{2} L p_x^2. \tag{35}$$

Applying (34) leads to the equations:

$$x = X - L p_x, \quad \text{and} \quad P_x = p_x. \tag{36}$$

In this case, the equations are easily solved to give explicit expressions for $X$ and $P_x$ in terms of $x$ and $p_x$.

In more general cases, the equations (34) need to be solved numerically each time the transfer map needs to be applied.

Lie transformations make use of the fact that the equations of motion for a particle in an electromagnetic field can be written in the form:

$$\frac{d\vec{x}}{ds} = -:H:\vec{x}, \tag{37}$$

where $\vec{x} = (x, p_x, y, p_y, z, \delta)$ is the phase space vector, and $:H:$ is a Lie (differential) operator:

$$:H: = \sum_{i=1}^{3} \frac{\partial H}{\partial x_i}\frac{\partial}{\partial p_i} - \frac{\partial H}{\partial p_i}\frac{\partial}{\partial x_i}. \tag{38}$$

The precise form of the function $H = H(\vec{x})$ (the Hamiltonian) depends on the field.

Formally, a solution to (37) can be written:

$$\vec{x}|_{s=L} = e^{-L:H:}\,\vec{x}|_{s=0}\,, \tag{39}$$

where the exponential of the Lie operator is defined by its series expansion.

The operator $e^{-L:H:}$ is known as a *Lie transformation*.

Applying a Lie transformation to a phase space variable generally leads to an infinite power series.

However, the power of Lie transformations lies in the fact that:

- there are known mathematical rules for combining and manipulating Lie transformations, and
- for any *generator* $g = g(\vec{x})$ the Lie transformation $e^{:g:}$ represents a symplectic map.